



Cite this: *RSC Adv.*, 2017, 7, 31212

# Self-healable hydrogels with NaHCO<sub>3</sub> degradability and a reversible gel–sol–gel transition from phenolic ester containing polymers†

Heng An,<sup>a</sup> Xu Li,<sup>a</sup> Xuehong Fu,<sup>a</sup> Juan Hu,<sup>a</sup> Xiaojie Lang,<sup>a</sup> Xiaoyu Liu,<sup>a</sup> Yong Wang,<sup>b</sup> Haijun Wang,<sup>a</sup> Ruixue Chang<sup>a</sup> and Jianglei Qin <sup>\*a</sup>

Due to their fantastic self-healing property, similar to that of organisms, self-healable hydrogels have attracted considerable attention in recent years. Herein, self-healable hydrogels with degradability in NaHCO<sub>3</sub> were prepared and showed a reversible gel–sol–gel transition under a variety triggers. The hydrogel was prepared from poly(*N,N*-dimethylacrylamide-*stat*-4-formylphenyl acrylate), P(DMA-*stat*-FPA), and dihydrazide with dynamic acylhydrazone and disulfide cross-linking. With base labile phenolic ester bond connections, the hydrogel can be degraded by the extremely mild base, NaHCO<sub>3</sub> solution. With a dihydrazide compound as a cross-linker, the hydrogel formed and self-healed without any additional catalysis or stimulus. Moreover, the self-healable hydrogels showed a reversible gel–sol–gel transition under various conditions, including pH, redox and group ratios, based on the reversible characteristics of acylhydrazone and disulfide bonds. With these superior properties, the developed hydrogel holds great potential for applications in many biomedical fields, including tissue engineering, drug delivery carriers and biosensors.

Received 25th May 2017

Accepted 9th June 2017

DOI: 10.1039/c7ra05854c

rsc.li/rsc-advances

## Introduction

The self-healing and self-repairing property is the ability to heal spontaneously after damage, and is one of the most fascinating characteristics of living creatures compared to their non-living counterparts. Accordingly, living creatures can repair damage to their organs when alive, and the self-healing property vanishes after their death. This fascinating self-healing feature has inspired researchers to design self-healable artificial materials to mimic the self-healing process of living creatures. As a result, the study of self-healable materials has made great progress based on both chemical and physical cross-linking in the past decade.<sup>1–7</sup> Accordingly, these materials are defined as self-healable chemical<sup>6</sup> and physical materials<sup>8–15</sup> respectively.

Besides physical cross-linked ones, self-healable materials based on dynamic chemical bonds have improved dimensional stability and solvent resistance. The reversible Diels–Alder reaction under heating, the cycloaddition reaction of cinnamate and reshuffling reaction of trithiocarbonates under UV triggers are used to prepare self-healable polymer materials.<sup>2,16,17</sup> The Cheng group designed dynamic urea bonding for reversible

cross-linking to prepare self-healable polymer materials, and a self-healable polymer material containing carboxylate/amine bonds and bulky *N*-substituents was designed.<sup>5</sup> Imato *et al.* had reported dynamic materials with diarylbibenzofuranone employed as a dynamic covalent unit, and the polymer material can self-heal its cracks at room temperature.<sup>18</sup> A series of imine bonds (Schiff-base) based on reversible reaction of amido group and carbonyl group were also applied to prepare self-healable materials and gels as reported.<sup>19–21</sup> The self-healable hydrogel containing reversible oxime bond was prepared from P(DMA-*stat*-DAA) with propanediylbishydroxylamine dihydrochloride as cross-linker, which can be degraded by monofunctional alkoxyamine.<sup>22</sup> Deng *et al.* designed novel self-healable polymeric gels based on dynamic covalent bond of acylhydrazone, the gels showed gel–sol–gel transition under various acidity and drawn great attentions.<sup>23–25</sup> Thermo-responsive hydrogel based on acylhydrazone were also reported in our previous publication.<sup>26</sup> Other self-healable polymer materials and gels with disulfide bond with redox reversibility,<sup>27</sup> boronic esters bond were also published in the past few years.<sup>28,29</sup> Among above self-healable materials and gels, the real “self-healable” property without any additional stimulus or triggers similar to that of organisms are greatly preferred for bio-applications, and this property can help us to understand the self-healing mechanism of living creatures. Hydrogels based on acylhydrazone can be formed and self-healed without any stimulus in water; on the other hand, the hydrazide group would not react with the ester group. These properties endows the acylhydrazone containing

<sup>a</sup>College of Chemistry and Environmental Science, Hebei University, Baoding 071002, China. E-mail: qinhbu@iccas.ac.cn

<sup>b</sup>College of Basic Medical Science, Hebei University, Baoding 071002, China

† Electronic supplementary information (ESI) available: DSC curves of copolymers, photographs of hydrogels with different component and gel–sol transitions under different conditions. See DOI: 10.1039/c7ra05854c



self-healable materials with great potential application in bioscience and biotechnology.

Besides self-healing property, degradability is a very important property for synthetic polymer materials, especially for cross-linked materials. The degradation of the materials can avoid by-effects after their tasks are completed. Although the dynamic covalent bonds and the active ester bonds can be degraded under certain stimulus by their nature,<sup>24,30–32</sup> the conditions are not mild or bio-compatible enough. As a result, degradable self-healable material are rarely reported. There were some publications about degradable self-healable polymer material reported recently, but the degradation of the network is still based on the reversible reaction of Schiff-base.<sup>19,33</sup> As a result, large amount of solvent or acid is required to dilute the gelator or consume the amine. Based on our previous study, the phenolic ester bond is extremely basic labile that can be cleaved by  $\text{NaHCO}_3$ .<sup>34</sup> When the phenolic ester was imported into the self-healable hydrogel, it is possible to prepare novel self-healable hydrogel that can be degraded under extremely mild base. We have reported self-healable organic polymer gels that can be degraded in  $\text{Na}_2\text{CO}_3$  solutions,<sup>35</sup> but the self-healable hydrogel that can be degraded by  $\text{NaHCO}_3$  has not studied up to now.

In this work, self-healable hydrogels were prepared based on water soluble P(DMA-*stat*-FPA) with pendant aldehyde group *via* phenolic ester connection. Result showed that self-healable hydrogels with reversible gel–sol–gel transition were prepared successfully based on dynamic acylhydrazone bond. Moreover, the hydrogels can be degraded by extremely mild base of  $\text{NaHCO}_3$ . To the best of our knowledge, there is no precedent report on the degradation of self-healing hydrogels based on cleavage of phenolic bond in extremely mild base of  $\text{NaHCO}_3$ . This kind of degradable self-healable hydrogel without addition of catalyst have improved potential applications and bio-safety in bioscience fields, such as tissue engineering, drug delivery carriers, biosensors, *etc.*

## Experimental

### Materials

*N,N*-Dimethylacrylamide (DMA), dimethyl 3,3'-dithiodipropionate, DL-dithiothreitol (DTT) and adipic dihydrazide (ADH) were purchased from Macklin biochemical Co Ltd. DMA was passed through a short column filled with basic alumina to remove inhibitor prior to copolymerization. 3,3'-Dithiobis(propionohydrazide)dithiodipropionic acid dihydrazide (DTDPH) was synthesized from dimethyl 3,3'-dithiodipropionate according to literature.<sup>24</sup> 4-Hydroxybenzaldehyde, acryloyl chloride, tosyl chloride were purchased from Maya Reagent Co. Poly(ethylene oxide) (PEO, DP = 45, 90 and 227 separately) were supplied by Guangfu Fine Chemical Research Institute and used to prepare PEO dihydrazide (PEO DH) according to literature.<sup>23</sup> The chain transfer agent S-1-dodecyl-S'-(R,R'-dimethyl-R''-acetic acid) tri-thiocarbonate (DDMAT) was synthesized according to previous report.<sup>36</sup> 2,2'-Azobisisobutyronitrile (AIBN, Kermel, 99%) was recrystallized in ethanol twice before use. Other chemicals including hydrazine hydrate, 80%,  $\text{H}_2\text{O}_2$ , HCl, triethylamine,

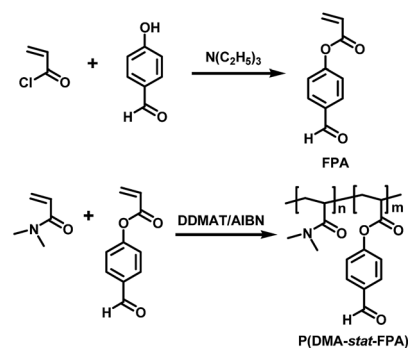
$\text{NaHCO}_3$ ,  $\text{Na}_2\text{CO}_3$ , anhydrous,  $\text{MgSO}_4$  and solvents (THF,  $\text{CH}_2\text{Cl}_2$ , toluene, dioxane, DMF, ethyl acetate, petroleum ether, *etc.*) were supplied by Kermel Chemical Reagent Co. and used as received.

### Characterizations

$^1\text{H}$  NMR characterization were carried out on a Bruker 600 MHz spectrometer (Avance III, Bruker); the samples were dissolved in  $\text{CDCl}_3$  and the characterization was performed at room temperature. A Varian 600 IR spectrometer was used to obtain the Fourier-transform infrared (FT-IR) spectra. The samples were dissolved in solvents and casted on a KBr plate for characterization. Gel permeation chromatography (GPC) characterization was performed with THF as the eluent and PS as the standard. The  $T_g$  of the copolymer was determined by differential scanning calorimetry (Diamond DSC, Perkin Elmer), the sample was heated to 200 °C and then cooled to 0 °C, the  $T_g$  value was collected from the second run at a heating rate of 20 °C  $\text{min}^{-1}$ . Thermogravimetric analysis (TGA) was carried out on a Pyris 1 instrument (Perkin Elmer), the samples were heated from 30 °C to 600 °C with a heating rate of 20 °C  $\text{min}^{-1}$  under  $\text{N}_2$  atmosphere. The lyophilized hydrogel samples were observed on a JSM-7500 field-emission scanning electron microscope (FE-SEM) with operating voltage of 10 kV and the images were recorded by a CCD camera. The samples were mounted on an aluminum specimen mounts and coated with Au for observations. The UV spectra of the monomer, copolymer and degraded products were scanned with a Shimadzu WV-2550 UV-vis spectrophotometer to compare the structure change under various conditions. Rheological properties of the hydrogels were measured on a TA AR2000ex rheometer with oscillatory mode at 25 °C.

### Synthesis of FPA and preparation of P(DMA-*stat*-FPA) through RAFT polymerization

The 4-formylphenyl acrylate (FPA) was prepared by the reaction of 4-hydroxybenzaldehyde with acryloyl chloride and purified according to our previous report and illustrated in Scheme 1 (top).<sup>4,35</sup> 4-Hydroxybenzaldehyde and acryloyl chloride were reacted in anhydrous  $\text{CH}_2\text{Cl}_2$  (DCM) with triethylamine as



Scheme 1 Synthesis of FPA and preparation of P(DMA-*stat*-FPA) through RAFT polymerization.



catalyst, the product of FPA was purified by silica gel chromatography and used for synthesis of functional copolymers.

The P(DMA-*stat*-FPA) with different compositions were prepared through RAFT copolymerization mediated by DDMAT with AIBN initiation. The procedure of the copolymerization is illustrated in Scheme 1 (bottom) and described as follows. DDMAT (72.8 mg, 0.2 mmol), DMA (2.18 g, 22 mmol), FPA (0.39 g, 2.2 mmol) and AIBN (4.9 mg, 0.06 mmol) were dissolved in 3 mL dioxane in a 25 mL reaction tube. The tube was sealed with a rubber plug and the oxygen in the mixture was removed through three freeze–pump–thaw cycles. Then the tube was immersed in a 60 °C oil bath and the polymerization was performed for 24 h under N<sub>2</sub> with continuous stirring.<sup>10,37–39</sup> The polymerization was stopped by opening the tube to air and cooled to room temperature, the product was precipitated in petroleum ether/ethyl acetate (8/2) three times and dried under vacuum. The molecular weight of the polymer was calculated based on the monomer conversion by weighing the product. The composition of P(DMA-*stat*-FPA) was calculated by comparing the corresponding peak areas on <sup>1</sup>H NMR spectrum.

### Thermal properties of the copolymer and the hydrogel

The DSC characterization was carried out to investigate the influence of the composition on *T*<sub>g</sub> of the copolymers. The samples were heated to 200 °C at 20 °C min<sup>-1</sup> and cooled to 0 °C, the heating curve of the second run was collected to obtain the *T*<sub>g</sub> value of the copolymers. The TGA characterizations were carried out to compare the stability of the copolymer and the strength of the chemical bonds, the samples were heated from room temperature to 600 °C at 20 °C min<sup>-1</sup> heating rate. The copolymer and freeze dried hydrogels were characterized to determine the decomposition temperature of the phenolic ester bond.

### Preparation of self-healable hydrogels

To study the hydrogel formation, the P(DMA-*stat*-FPA) copolymers with different compositions were dissolved in glass vials to form a homogeneous solution, then stoichiometric DTDPH or PEO dihydrazide solution as cross-linker was added into the vial. The vial was shaken at room temperature until a clear solution with total concentration of 10% was obtained. Then the solution was put into the round moulds to form hydrogel for self-healing and rheology studies, hydrogels formed in vials were used to determine the gel–sol–gel transition under a variety of triggers. Gel formation was confirmed by vial inversion and characterized by rheometry. Rheology tests and self-healing properties were investigated after clear hydrogel was formed and incubated for at least 24 h.

### Rheological investigation of hydrogel and mechanical properties

The rheological properties of the hydrogels were measured on a TA AR2000ex rheometer with an oscillating mode, parallel aluminum plate with 25 mm diameter was used for the characterizations. The gap was fixed between 800–1000 μm for all the measurements; the frequency scan was carried out from

0.03–100 rad s<sup>-1</sup> and the strain of 5% was selected within the linear viscoelastic regime. All measurements were conducted under N<sub>2</sub> protection.

### Self-healing study of hydrogels

Self-healing process of the hydrogels were carried out as follows: first, hydrogel was prepared in round mould in a sealed desiccator saturated with moisture. After incubated for 24 h, the gel plate was cut into two pieces across the center and put back into the original mould with cutting surfaces contacted closely. The mould was put back into the desiccator again and incubated for 24 h in saturated moisture. Self-healing results was confirmed by subjecting to gravity and stretching the healed hydrogel with tweezers from both sides perpendicular to the cutting line. The experiment was repeated by cutting the healed hydrogel in a perpendicular direction. Each time the healed hydrogel was incubated for 24 h before being cut again.

### UV-vis absorbance of the FPA, P(DMA-*stat*-FPA) and the degraded product

The UV spectra of the copolymer under different conditions were obtained on a Shimadzu WV-2550 UV-vis spectrophotometer with the scanning range of 200–600 nm wavelengths. To compare the cleavage of the phenolic ester bond, 10 mg of P(DMA<sub>10.4</sub>-*stat*-FPA<sub>8</sub>) was dissolved in 1 mL 2% NaHCO<sub>3</sub> and Na<sub>2</sub>CO<sub>3</sub> solution respectively and stirred for 24 h, then UV-vis characterization were carried out after diluted to proper concentration. The degraded hydrogel was also characterized after dilution.

### Morphology of the hydrogel through SEM observation

To observe the morphology of the self-healable hydrogels, the hydrogel samples were lyophilized and fractured in liquid nitrogen to preserve the original morphology. The fracture surfaces were observed by a JSM-7500 FE-SEM after coated with Au. The morphology and the cross-linking density of the hydrogels were compared by examination of the SEM images.

### Gel–sol–gel transition under a variety of reversible triggers

To investigate the acid responsiveness of the hydrogel, CF<sub>3</sub>CO<sub>2</sub>H, HCl (5 M) was dropped onto the top of the hydrogel in a vial. The appearance change was visualized at different time intervals to monitor the gel–sol transition. After the hydrogel was dissolved, triethylamine was added to neutralize the acid with shaking and the gel–sol–gel transitions were recorded with a digital camera. The other hydrogels were investigated in the same process.

The disulfide bond is reversible under redox, which can endow the hydrogel with redox induced gel–sol–gel transition and self-healing properties.<sup>27</sup> 3 equivalent of DTT based on disulfide bond was added into the hydrogel with DTDPH as cross-linker and shook continuously to visualize the gel–sol transition. After the hydrogel was transitioned into liquid, stoichiometric H<sub>2</sub>O<sub>2</sub> was added to investigate the sol–gel transition and the process was recorded by a digital camera.



The reversible acylhydrazone exchange can also be performed between hydrogel and excess of dihydrazine compounds to obtain linear polymer with pendant hydrazine groups. 3 times equivalent of dihydrazine in water solution (10%) was added into the hydrogel and the vial was shaken periodically to observe the gel-sol transition. After the hydrogel was transformed into a clear solution, P(DMA-*stat*-FPA) in 10% solution was added to regulate the group ratio to 1 : 1, the hydrogel formation was observed and recorded with a digital camera.

### Degradation of self-healable hydrogels under mild base

The degradation of the hydrogels with phenolic ester cross-linking were carried out as follows: the NaHCO<sub>3</sub> solution (0.22 g 10%) was dropped on the hydrogel in a glass vial (1 g with 10% gelator) to regulate the resultant NaHCO<sub>3</sub> concentration of 2%. The degradation of the hydrogel was confirmed by leaning the vial compared to as prepared hydrogel. The degraded solution was diluted and scanned by UV-vis spectrometer to compare the UV spectrum with the copolymer.

## Result and discussion

### Synthesis of 4-formylphenyl acrylate and polymerization of P(DMA-*stat*-FPA)

The FPA was synthesized by reaction of 4-hydroxybenzaldehyde and acryloyl chloride in DCM according to our previous report,<sup>35</sup> and the structure was characterized by <sup>1</sup>H NMR. Polymerization of P(DMA-*stat*-FPA) was initiated by AIBN and mediated by DDMAT (Scheme 1). The molecular weight of the copolymer was

evaluated by monomer conversion and the composition of the copolymer was determined by <sup>1</sup>H NMR. The <sup>1</sup>H NMR spectra of FPA and P(DMA<sub>104</sub>-*stat*-FPA<sub>8</sub>) are shown in Fig. 1. The peak c (7.91 ppm) and e (9.97 ppm) on spectrum of P(DMA<sub>104</sub>-*stat*-FPA<sub>8</sub>) were originated from FPA, the peak g (2.91 ppm) was derived from DMA, which confirmed the copolymerization reaction, as shown in Fig. 1 (bottom). The composition of the copolymer was calculated by comparing the peak area of c (7.91 ppm) and g (2.91 ppm). Based on the <sup>1</sup>H NMR results, the composition of FPA were lower than monomer feeding ratio and two samples with different compositions were synthesized for comparison, as listed in Table 1.

The structures of FPA and copolymers were also characterized by FT-IR. Two absorbances appeared at 1744 cm<sup>-1</sup> and 1700 cm<sup>-1</sup> represented carbonyl groups of ester bond and aldehyde group respectively, as shown in Fig. 2 (top). The absorbance at 1600 cm<sup>-1</sup> on the spectrum is derived from benzene ring, which proved the structure of FPA. After copolymerization, three absorbance peaks representing carbonyl groups are illustrated at 1757 cm<sup>-1</sup>, 1700 cm<sup>-1</sup> and 1645 cm<sup>-1</sup> separately, as shown in Fig. 2 (bottom). The absorbance at 1645 cm<sup>-1</sup> is derived from amide group on DMA segment; while the other two peaks are come from FPA. It was also noticed that the absorbance of ester carbonyl group on FPA moved to 1757 cm<sup>-1</sup> because the C=C bond was consumed during the copolymerization. Although the size of FPA segment is much bigger than that of DMA, the T<sub>g</sub> of the copolymers decreased with increasing FPA composition because of decreased H-bond force, as determined by DSC (Fig. S1†), the T<sub>g</sub> values of the copolymer are listed in Table 1.

### Preparation of hydrogels from P(DMA-*stat*-FPA) with a variety of dihydrazine cross-linking

The reversible acylhydrazone bond can be formed automatically in water conditions without any additional catalysis or stimulus,<sup>26</sup> which endows the acylhydrazone based self-healable hydrogels with better bio-compatibility and better persistence. On the other hand, the stimulus free self-healing process can be used in more areas without worrying about run away of catalyst. The hydrogels were prepared in deionized water to investigate the gelation reaction and the group ratio of aldehyde to hydrazide was fixed at 1 : 1, the formation of hydrogel was confirmed by tilting the vials.

The hydrogels were prepared by reaction of P(DMA-*stat*-FPA) with dihydrazide compounds, the dihydrazide with various molecular weights were used to regulate the cross-linking density and composition of the hydrogels, as shown in

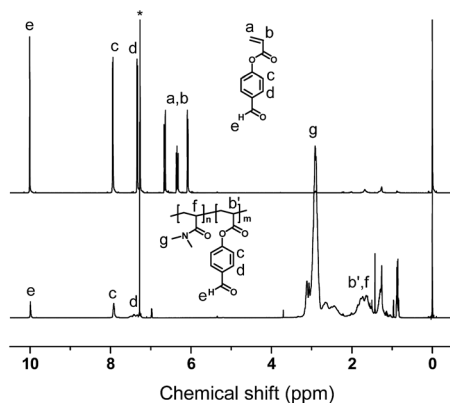


Fig. 1 <sup>1</sup>H NMR spectra of FPA (top) and P(DMA<sub>104</sub>-*stat*-FPA<sub>8</sub>) in CDCl<sub>3</sub> (bottom).

Table 1 Copolymers of P(DMA-*stat*-FPA) with different compositions

Sample	Polymer	FPA molar ratio <sup>a</sup>	M <sub>n</sub> <sup>b</sup> (kg mol <sup>-1</sup> )	M <sub>w</sub> /M <sub>n</sub> <sup>c</sup>	T <sub>g</sub> (°C)
P1	P(DMA <sub>199</sub> - <i>stat</i> -FPA <sub>4</sub> )	2%	21.8	1.18	119.1
P2	P(DMA <sub>104</sub> - <i>stat</i> -FPA <sub>8</sub> )	7%	11.7	1.17	105.6

<sup>a</sup> Calculated from <sup>1</sup>H NMR spectroscopy. <sup>b</sup> Evaluated by monomer conversion. <sup>c</sup> Determined by GPC.



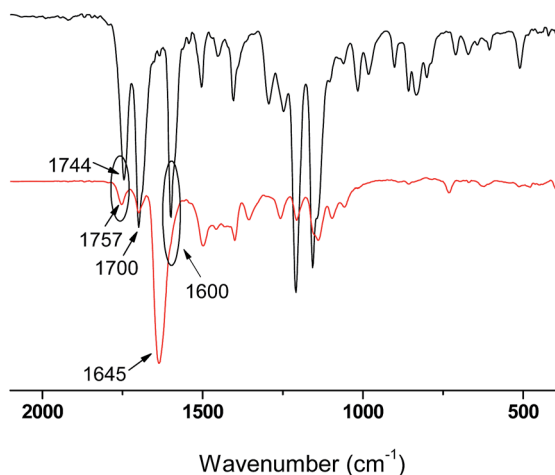
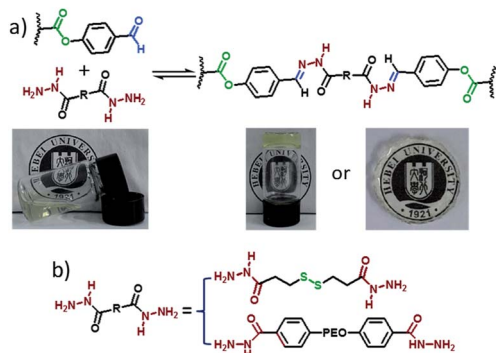


Fig. 2 FT-IR spectra of FPA (top) and P(DMA<sub>104</sub>-stat-FPA<sub>8</sub>) (bottom).

Scheme 2. It was noted the hydrogel prepared from P(DMA<sub>199</sub>-stat-FPA<sub>4</sub>) cross-linked by DTDPH is actually a viscous sol because of its low stiffness (Fig. S2†). The hydrogels prepared from P(DMA<sub>104</sub>-stat-FPA<sub>8</sub>) with DTDPH as cross-linkers formed in several minutes without any addition stimulus (Scheme 2). Moreover, the density of cross-linking point can be regulated by increasing the  $M_n$  of cross-linker. When the cross-linker was changed into PEO dihydrazide with various molecular weights, all the hydrogels formed within 1 h. The mechanical properties of the hydrogels with different cross-linking densities and composition of gelator can then be examined.

### Rheological properties of self-healable hydrogels

The mechanical properties of the hydrogels were determined by rheology characterization, the storage modulus ( $G'$ ), loss modulus ( $G''$ ) and complex viscosity ( $\eta^*$ ) dependant on frequency were determined. The P(DMA<sub>199</sub>-stat-FPA<sub>4</sub>) cross-linked by DTDPH is actually a viscous sol. With increasing functionality, the hydrogel prepared from P(DMA<sub>104</sub>-stat-FPA<sub>8</sub>) and DTDPH showed solid characteristic that the  $G' > G''$  in whole frequency range and the  $G'$  is very low, which indicated



Scheme 2 Schematic illustration for preparation of hydrogel from P(DMA-stat-FPA) with dihydrazide cross-linking (a) and the structure of the dihydrazide cross-linkers (b). (Credit from Hebei University).

the low strength of the hydrogel, as shown in Fig. 3a. It is surprising to notice that the  $G'$  increased and then decreased with increasing  $M_n$  of the PEO dihydrazide cross-linkers, when the PEO<sub>45</sub> dihydrazide ( $M_n = 2270$ ) and PEO<sub>90</sub> dihydrazide ( $M_n = 4270$ ) were used as cross-linker, the  $G'$  increased gradually rather than decreasing although cross-linking density decreased, as shown in Fig. 3(b and c). When the cross-linker was further changed to PEO<sub>227</sub> dihydrazide ( $M_n = 10\ 270$ ), the  $G'$  decreased with the decrease in crosslink density (Fig. 3d). This result indicated that the strength of the hydrogel ( $G'$ ) depends not only on cross-linking density, but also on composition of the gelators and the PEO can increase the strength of the hydrogel. Importantly, all samples showed solid characteristic that with  $G' > G''$ . This result was confirmed through cross-linking P(DMA<sub>199</sub>-stat-FPA<sub>4</sub>) by PEO<sub>90</sub> dihydrazide, as expected, hydrogel with increased strength was obtained (Fig. S3†)

### Self-healing study of the hydrogels with various cross-linking densities

The self-healing properties of hydrogels with various compositions and cross-linking agents were studied, however, the hydrogels prepared from P(DMA<sub>104</sub>-stat-FPA<sub>8</sub>) cross-linked by DTDPH with the highest cross-linking density was sticky and soft as characterized by rheology; as a result, the self-healing experiment can not be carried out. When PEO<sub>45</sub> dihydrazide was used as cross-linker, although the cross-linking density decreased, the hydrogel was no longer sticky and the self-healing performed perfectly. The self-healing process of this hydrogel is shown in Fig. 4-1, when the hydrogel (Fig. 4-1a) was cut into two halves across the center (Fig. 4-1b) and put back into the original mould with close contact, the hydrogel self-healed *via* acylhydrazone exchange without any stimulus (Fig. 4-1c) and cannot split under stretching (Fig. 4-1d). Moreover, the self-healing can be repeated with no difference noticed (Fig. S4†). However, with further increasing  $M_n$  of cross-linker,

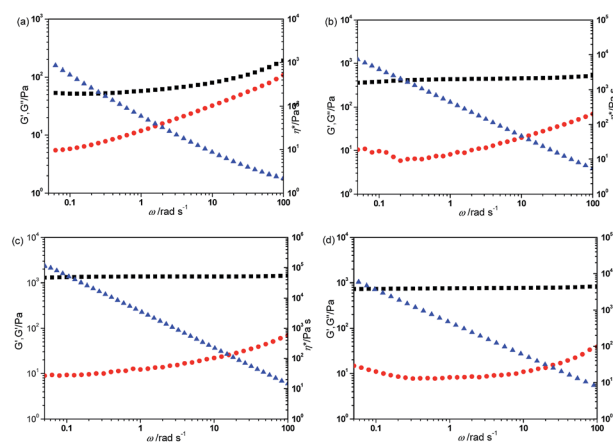


Fig. 3 Rheological experiments of P(DMA<sub>104</sub>-stat-FPA<sub>8</sub>) copolymers with various cross-linking agent. The gelator concentrations are 10% and the group ratio of 1 : 1 (5% strain, and 25 °C). (a) DTDPH; (b) PEO<sub>45</sub> dihydrazide; (c) PEO<sub>90</sub> dihydrazide; (d) PEO<sub>227</sub> dihydrazide. (Black:  $G'$ ; red:  $G$ ; blue:  $\eta^*$ ).



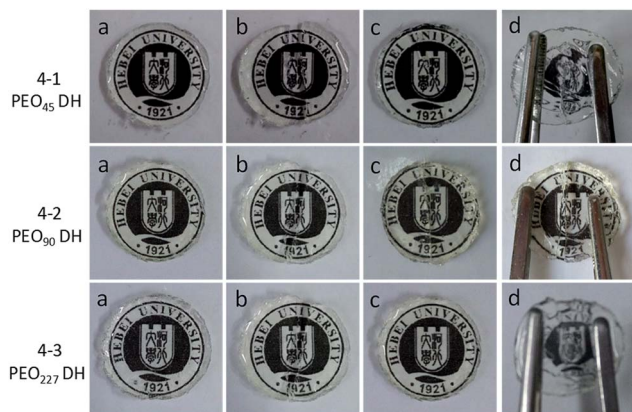


Fig. 4 Self-healing study of the hydrogels prepared from P(DMA<sub>104</sub>-*stat*-FPA<sub>8</sub>) with various PEO dihydrazide (PEO DH) cross-linking. (Credit from Hebei University).

the hydrogel cross-linked by PEO<sub>90</sub> dihydrazide did not self-heal in 24 h (Fig. 4-2(a-d), and even in 72 h). This result is surprising because the lower cross-linking density should facilitate the movement of the polymer chains. Based on the rheological study, the  $G'$  of this hydrogel is higher than that with PEO<sub>45</sub> dihydrazide cross-linking. This result indicated that the reversible reaction depends on stiffness of hydrogel besides cross-linking density, and high stiffness restricted the reversible reaction of the acylhydrazone along the cut line. When the molecular weight of the cross-linker further increased, the hydrogel with PEO<sub>227</sub> dihydrazide cross-linking become self-healable again, as shown in Fig. 4-3(a-d).

### Morphology of the hydrogels

The cross-linking density of the hydrogels was compared by SEM. The hydrogels were freeze dried directly to preserve the original morphology. The SEM images of the hydrogels are shown in Fig. 5. As shown in Fig. 5a, although the stiffness of the hydrogel with DTDPH cross-linking was comparatively low, the regular micro pores with uniform pore size of 3–5  $\mu\text{m}$  are illustrated in the picture. When the cross-linker was changed to PEO dihydrazide, the pore size increased with increasing  $M_n$  of the cross-linker and the pore walls collapsed, as shown in Fig. 5b and c. The possible reason for this result is the morphology changed after fracture since the observation temperature was much higher than  $T_g$  of PEO and the PEO ratio in the hydrogels were pretty high.

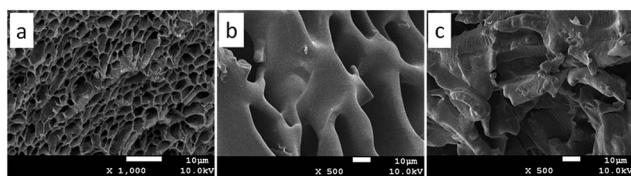


Fig. 5 SEM photographs of hydrogels after freeze dried from P(DMA<sub>104</sub>-*stat*-FPA<sub>8</sub>) cross-linked by DTDPH (a), PEO<sub>45</sub> dihydrazide (b) and PEO<sub>90</sub> dihydrazide (c).

### Gel-sol-gel transition and degradation of the hydrogels in mild base

The acylhydrazone bond can go reversible coupling and decoupling reaction under pH triggers, so the hydrogel can go gel-sol transition by regulating the pH of the water. When CF<sub>3</sub>COOH was added into the hydrogel, all hydrogels were dissolved into liquid fluid overnight, the same result was obtained with addition of 5 M HCl to change the pH to 3. The pH triggered gel-sol transition of hydrogel with PEO<sub>45</sub> dihydrazide cross-linking is shown in Fig. 6. When the pH of the solution was changed to 6.5 by addition of triethylamine, the hydrogel was obtained again, as shown in Fig. 6(a and b). Above result confirmed that the phenolic ester is pretty stable under mild acid at room temperature. With base labile phenolic ester bond on the copolymer structure, the hydrogel also showed gel-sol transition in mild base, when Na<sub>2</sub>CO<sub>3</sub> solution was added into the self-healable hydrogel to 2% concentration, the hydrogel degraded gradually within 24 h and the resultant solution became brown, as shown in Fig. 6c. The NaHCO<sub>3</sub> can also degrade the hydrogel, but because of low reactivity of NaHCO<sub>3</sub>, the degradation of the hydrogel need pretty long time scale. The NaHCO<sub>3</sub> solution was absorbed and the hydrogel turned brown after 3 days, and the hydrogel degraded gradually into dark brown viscous liquid in two weeks, as shown in Fig. 6 (bottom), this result also proved the phenolic ester bond in conjugated structure can still be cleaved by NaHCO<sub>3</sub>, but the degradation rate is very slow. Further experiments showed that excess triethylamine can also degrade the hydrogels (Fig. S5†). It is easy to understand the hydrogel cannot be obtained by regulating the pH of the solution to neutral since the phenolic ester connection was cleaved, as shown in Scheme 3. Other hydrogels also showed the same result because of same cross-linking structure.

The degradation of phenolic ester bond was tracked and confirmed by UV characterizations. The UV spectra of the P(DMA<sub>104</sub>-*stat*-FPA<sub>8</sub>), its degradation products in NaHCO<sub>3</sub> and Na<sub>2</sub>CO<sub>3</sub> along with degraded self-healable hydrogel with PEO<sub>45</sub> dihydrazide cross-linking are shown in Fig. 7. The copolymer showed the absorbance at 253 nm, as shown in Fig. 7 (black line). After stirred in Na<sub>2</sub>CO<sub>3</sub> for 24 h, the peak at 253 nm disappeared completely because the phenolic ester bond was cleaved (Fig. 7 blue line). However, the phenolic ester bond was only cleaved partially in NaHCO<sub>3</sub> in 24 h and the peak at 253 nm

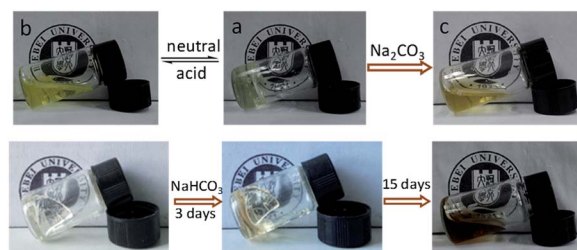
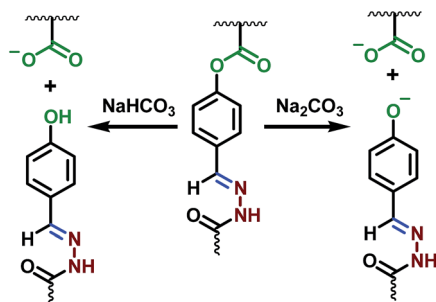


Fig. 6 pH triggered gel-sol-gel transition and degradation in Na<sub>2</sub>CO<sub>3</sub> of the self-healable hydrogel prepared from P(DMA<sub>104</sub>-*stat*-FPA<sub>8</sub>) with PEO<sub>45</sub> dihydrazide cross-linking (top) and degradation process of the hydrogel in NaHCO<sub>3</sub> (bottom).





Scheme 3 Schematic illustration for degradation of hydrogel in  $\text{NaHCO}_3$  and  $\text{Na}_2\text{CO}_3$ .

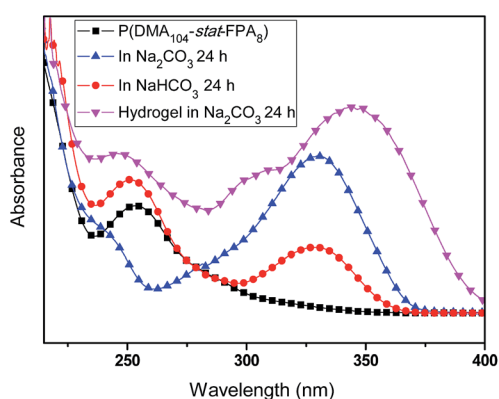


Fig. 7 UV spectra of  $\text{P}(\text{DMA}_{104}\text{-stat-FPA}_8)$  and its degradation products in 2%  $\text{NaHCO}_3$ ,  $\text{Na}_2\text{CO}_3$  and degraded hydrogel with  $\text{PEO}_{45}$  dihydrazide cross-linking for 24 h in  $\text{Na}_2\text{CO}_3$ .

was still exist (Fig. 7 red line). The self-healable hydrogel can be degraded in  $\text{NaHCO}_3$  and  $\text{Na}_2\text{CO}_3$ , but the UV spectrum showed the phenolic ester bond in the hydrogel only degraded partially in  $\text{Na}_2\text{CO}_3$  in 24 h without stirring and some absorbance was still existed at 253 nm, as shown in Fig. 7 (purple line). Moreover, the absorbance of the degradation product moved to 344 nm because the aldehyde group had reacted with hydrazide and changed the conjugated structure.

As the disulfide bond can be cleaved by reduction, the hydrogel with DTDPH cross-linking also go redox triggered gel-sol-gel transition besides pH triggered gel-sol-gel transition, as shown in Fig. 8(a-c). When 2 equivalents of DTT was added into

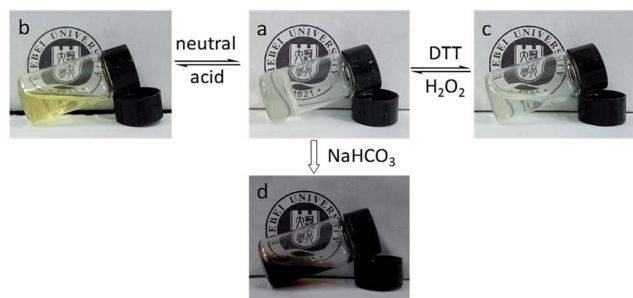


Fig. 8 Gel-sol-gel transition and degradation of DTDPH cross-linked hydrogel.

the hydrogel with DTDPH cross-linking, the hydrogel was degraded into a viscous solution in 24 h because the disulfide group was reduced into thiol group. When same equivalent of  $\text{H}_2\text{O}_2$  was added to oxidize the thiol group, hydrogel was re-obtained since the disulfide group was formed again. With phenolic ester bond connection, this hydrogel was also degraded into a dark brown liquid by  $\text{NaHCO}_3$ , as shown in Fig. 8(d). However, although the hydrogel cross-linked by DTDPH showed multi-triggered gel-sol-gel transitions and  $\text{NaHCO}_3$  degradation, the low strength of this sample could limit its application in wide areas, multi-responsive self-healable hydrogel with improved strength and degradability in  $\text{NaHCO}_3$  is under intensive study.

It was reported that the self-healable hydrogels can be cleaved by group exchange with excess of mono-functional compound<sup>22</sup> and cross-linkers. The gel-sol-gel transition regulated by excess of dihydrazide compounds was investigated. When 3 equivalents excess of cross-linker was added into the hydrogel, the hydrogel was dissolved slowly in 24 h; moreover, when same equivalent of  $\text{P}(\text{DMA}_{104}\text{-stat-FPA}_8)$  was added to regulate the group ratio to 1 : 1, hydrogel was obtained again. The mechanism of this reaction and the photograph for this process are shown in Fig. 9. More importantly, although the hydrogel with  $\text{PEO}_{90}$  dihydrazide cross-linking did not self-heal within 72 h, this hydrogel still showed group ratio triggered gel-sol-gel transition (Fig. S6†) and other hydrogels showed the same result. Above result indicated that although the hydrogel with  $\text{PEO}_{90}$  dihydrazide cross-linking did not self-heal in 24 h, the reversible characteristic of acylhydrazone was still exist. But the acylhydrazone exchange rate was comparatively low along the cut line because high stiffness of the hydrogel restricted the movement functional group and polymer chain.

As mentioned above, the hydrogels can also be degraded by triethylamine. It was also noticed the hydrogel cannot be obtained again when the concentration of  $\text{HCl}$  was higher than  $0.1 \text{ mol L}^{-1}$  because the ester bond can also be cleaved by acid. On the other hand, when excess of  $\text{H}_2\text{O}_2$  was added to oxidize thiol group to disulfide group, the re-obtained hydrogel would degrade again. But the group ratio triggered gel-sol-gel transition never fail because no any possible side reaction involved in this process. Moreover, this process did not change any valency of the gelators nor produce any by-product. So this property provide a effective method to reuse and recycle of the self-healable hydrogel.

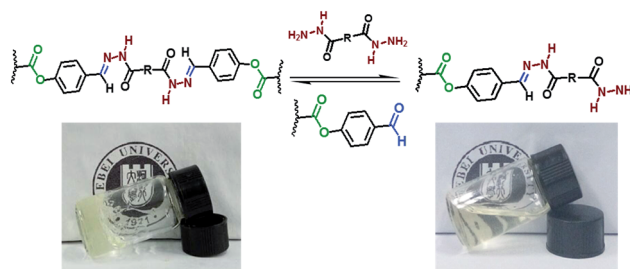


Fig. 9 Mechanism for group ratio triggered gel-sol-gel transition and photograph of the hydrogel prepared from  $\text{P}(\text{DMA}_{104}\text{-stat-FPA}_8)$  and  $\text{PEO}_{45}$  dihydrazide.



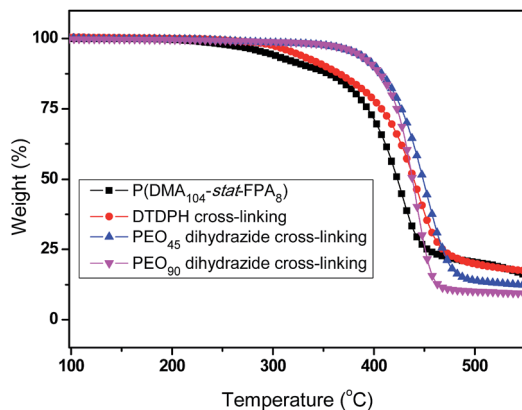


Fig. 10 TGA curves of the copolymer and the hydrogels with various cross-linking agents.

### Thermal stability of the copolymer and the hydrogels

The phenolic ester bond are less stable than other chemical bonds in the polymer chain, this property can be determined by TGA. The TGA curves of the copolymer and the hydrogels are shown in Fig. 10. The P(DMA<sub>104</sub>-stat-FPA<sub>8</sub>) began to loss some weight at 215 °C because the phenolic ester bond was cleaved and the 4-hydroxybenzaldehyde was evaporated, as shown Fig. 10 (black line), while the decomposition temperature of the polymer chain was much higher (>360 °C). After cross-linked by DTDPH, the decomposition temperature increased to 282 °C (red line in Fig. 10). Although the decomposition temperature of the phenolic ester bond should not change obviously, but the aldehyde has reacted with hydrazide group and can only evaporate with the cross-linker. On the other hand, there is no weight loss noticed at the decomposition of copolymer, indicated that there was no free aldehyde group left after cross-linking, proved the equilibrium constant of the coupling reaction is pretty high. When the PEO dihydrazide was used as cross-linker, no weight loss was noticed until 332 °C (Fig. 10 blue and purple line). This result is reasonable because there is no small molecules evaporate even if the phenolic ester bond was cleaved. There is only one weight loss process on the TGA curve, indicated the decomposition temperature of PEO and polymer chains are at the same temperature range.

Based on above studies, self-healable hydrogels with multi-triggered gel-sol-gel transition and basic degradation is designed, the degradation of the self-healable hydrogel is triggered by extremely mild base of NaHCO<sub>3</sub>. This kind of smart hydrogel could have great potential application in areas related to bioscience and biotechnology with enhanced persistence and can be degraded under mild conditions to avoid possible side effects. The application of this kind of self-healable hydrogel in drug loading and delivery is under investigation.

## Conclusion

Self-healable hydrogels were prepared from P(DMA-*stat*-FPA) cross-linked by dihydrazide compounds. With aldehyde group and phenolic ester bond in the P(DMA-*stat*-FPA), self-healable

hydrogel with NaHCO<sub>3</sub> degradability was prepared without any additional stimulus in purified water. The self-healable hydrogel showed gel-sol-gel transition based on reversible characteristics of acylhydrazone bond. The redox triggered gel-sol-gel transition can be realized with disulfide containing cross-linker. However, the PEO dihydrazide tends to increase the strength of the hydrogel although cross-linking density decreased. The hydrogel can be cleaved into solution with excess of cross-linker, which is very useful for recycle of the self-healable hydrogel. Importantly, the self-healable hydrogel can be degraded by mild base of NaHCO<sub>3</sub> through cleavage of the base labile phenolic ester bond.

## Acknowledgements

This research was kindly supported by Natural Science Foundation of Hebei (B2015201085); the Department of Education, Hebei Province (No. QN2017014); the Returned Overseas Chinese Scholars, State Education Ministry and Challenge Cup Program of Hebei University.

## References

- 1 J. Ling, M. Z. Rong and M. Q. Zhang, *Polymer*, 2012, **53**, 2691–2698.
- 2 C.-M. Chung, Y.-S. Roh, S.-Y. Cho and J.-G. Kim, *Chem. Mater.*, 2004, **16**, 3982–3984.
- 3 B. Ghosh and M. W. Urban, *Science*, 2009, **323**, 1458–1460.
- 4 N. Kuhl, S. Bode, R. K. Bose, J. Vitz, A. Seifert, S. Hoepfner, S. J. Garcia, S. Spange, S. van der Zwaag, M. D. Hager and U. S. Schubert, *Adv. Funct. Mater.*, 2015, **25**, 3295–3301.
- 5 H. Ying, Y. Zhang and J. Cheng, *Nat. Commun.*, 2014, **5**, 3218.
- 6 L. Hu, X. Cheng and A. Zhang, *J. Mater. Sci.*, 2015, **50**, 2239–2246.
- 7 M. Vatankhah-Varnoosfaderani, S. Hashmi, A. GhavamiNejad and F. J. Stadler, *Polym. Chem.*, 2014, **5**, 512–523.
- 8 M. Zhang, D. Xu, X. Yan, J. Chen, S. Dong, B. Zheng and F. Huang, *Angew. Chem., Int. Ed.*, 2012, **124**, 7117–7121.
- 9 P. Cordier, F. Tournilhac, C. Soulie-Ziakovic and L. Leibler, *Nature*, 2008, **451**, 977–980.
- 10 T. Ueki, Y. Nakamura, R. Usui, Y. Kitazawa, S. So, T. P. Lodge and M. Watanabe, *Angew. Chem., Int. Ed.*, 2015, **54**, 3018–3022.
- 11 T. Ueki, R. Usui, Y. Kitazawa, T. P. Lodge and M. Watanabe, *Macromolecules*, 2015, **48**, 5928–5933.
- 12 A. Phadke, C. Zhang, B. Arman, C.-C. Hsu, R. A. Mashelkar, A. K. Lele, M. J. Tauber, G. Arya and S. Varghese, *Proc. Natl. Acad. Sci. U. S. A.*, 2012, **109**, 4383–4388.
- 13 J. Zhan, M. Zhang, M. Zhou, B. Liu, D. Chen, Y. Liu, Q. Chen, H. Qiu and S. Yin, *Macromol. Rapid Commun.*, 2014, **35**, 1424–1429.
- 14 G. Li, J. Wu, B. Wang, S. Yan, K. Zhang, J. Ding and J. Yin, *Biomacromolecules*, 2015, **16**, 3508–3518.
- 15 D. L. Taylor and M. in het Panhuis, *Adv. Mater.*, 2016, **28**, 9060–9093.
- 16 X. Chen, M. A. Dam, K. Ono, A. Mal, H. Shen, S. R. Nutt, K. Sheran and F. Wudl, *Science*, 2002, **295**, 1698–1702.



- 17 Y. Amamoto, J. Kamada, H. Otsuka, A. Takahara and K. Matyjaszewski, *Angew. Chem., Int. Ed.*, 2011, **50**, 1660–1663.
- 18 K. Imato, M. Nishihara, T. Kanehara, Y. Amamoto, A. Takahara and H. Otsuka, *Angew. Chem., Int. Ed.*, 2012, **51**, 1138–1142.
- 19 H. Li, J. Bai, Z. Shi and J. Yin, *Polymer*, 2016, **85**, 106–113.
- 20 B. Maiti, B. Ruidas and P. De, *React. Funct. Polym.*, 2015, **93**, 148–155.
- 21 Y. Zhang, L. Tao, S. Li and Y. Wei, *Biomacromolecules*, 2011, **12**, 2894–2901.
- 22 S. Mukherjee, M. R. Hill and B. S. Sumerlin, *Soft Matter*, 2015, **11**, 6152–6161.
- 23 G. Deng, C. Tang, F. Li, H. Jiang and Y. Chen, *Macromolecules*, 2010, **43**, 1191–1194.
- 24 G. H. Deng, F. Y. Li, H. X. Yu, F. Y. Liu, C. Y. Liu, W. X. Sun, H. F. Jiang and Y. M. Chen, *ACS Macro Lett.*, 2012, **1**, 275–279.
- 25 F. Yu, X. Cao, J. Du, G. Wang and X. Chen, *ACS Appl. Mater. Interfaces*, 2015, **7**, 24023–24031.
- 26 R. Chang, X. Wang, X. Li, H. An and J. Qin, *ACS Appl. Mater. Interfaces*, 2016, **8**, 25544–25551.
- 27 S. Y. An, S. M. Noh, J. H. Nam and J. K. Oh, *Macromol. Rapid Commun.*, 2015, **36**, 1255–1260.
- 28 J. J. Cash, T. Kubo, A. P. Bapat and B. S. Sumerlin, *Macromolecules*, 2015, **48**, 2098–2106.
- 29 O. R. Cromwell, J. Chung and Z. Guan, *J. Am. Chem. Soc.*, 2015, **137**, 6492–6495.
- 30 J. Kamada, K. Koynov, C. Corten, A. Juhari, J. A. Yoon, M. W. Urban, A. C. Balazs and K. Matyjaszewski, *Macromolecules*, 2010, **43**, 4133–4139.
- 31 Y. Shi, X. F. Wang, R. W. Graff, W. A. Phillip and H. F. Gao, *J. Polym. Sci., Part A: Polym. Chem.*, 2015, **53**, 239–248.
- 32 R. Chang and J. Qin, *Macromol. Chem. Phys.*, 2014, **215**, 1908–1914.
- 33 A. Chao, I. Negulescu and D. Zhang, *Macromolecules*, 2016, **49**, 6277–6284.
- 34 R. Chang, N. Li, J. Qin and H. Wang, *Polymer*, 2015, **60**, 62–68.
- 35 R. Chang, H. An, X. Li, R. Zhou, J. Qin, Y. Tian and K. Deng, *Polym. Chem.*, 2017, **8**, 1263–1271.
- 36 J. T. Lai, D. Filla and R. Shea, *Macromolecules*, 2002, **35**, 6754–6756.
- 37 B. Peng, Y. Liu, Y. Shi, Z. Li and Y. Chen, *Soft Matter*, 2012, **8**, 12002–12008.
- 38 D. X. Wu, X. H. Song, T. Tang and H. Y. Zhao, *J. Polym. Sci., Part A: Polym. Chem.*, 2010, **48**, 443–453.
- 39 Y. Shi, W. Zhu and Y. Chen, *Macromolecules*, 2013, **46**, 2391–2398.

